Novel Cost Model for Balancing Wind Power Forecasting Uncertainty

Jie YAN, Yongqian Liu, Furong Li, Chenghong Gu

Abstract — The intermittency of wind generation creates nonlinear uncertainties in wind power forecasting (WPF). Thus, additional operating costs can be incurred for balancing these forecasting deviations. Normally, large wind power penetration requires accurate quantification of the uncertainty-induced costs. This paper defines this type of costs as wind power uncertainty incremental cost (WPUIC) and wind power uncertainty dispatch cost (WPUDC), and it then formulates a general methodology for deriving them based on probabilistic forecasting of wind power. WPUIC quantifies the incremental cost induced from balancing the uncertainties of wind power generation. WPUDC is a balancing cost function with a quadratic form considering diverse external conditions. Besides, the risk probability (RP) of not meeting the scheduled obligation is also modelled. Above models are established based on a newly developed probabilistic forecasting model, varying variance relevance vector machine (VVRVM). Demonstration results show that the VVRVM and RP provide an accurate representation of WPF uncertainties and corresponding risk, and thus they can better support and validate the modelling of WPUDC and WPUIC. The proposed cost models have the potential to easily extend traditional dispatches to a new low-carbon system with a high penetration of renewables.

Keywords—economic dispatch, forecasting incremental cost, uncertainty cost, wind power generation, wind power forecasting.

I. NOMENCLATURE ABBREVIATIONS

CDF	Cumulative distribution function
EIP	Energy imbalance prices
NWP	Numerical weather prediction
PDF	Probability density function
RMSE	Root mean square error
RP	Risk probability

RP

Relevance vector machine **RVM**

SBP System buy price **SSP** System sell price **VVRVM** Variable variance RVM WPF Wind power forecasting

WPPF Wind power probabilistic forecasting **WPUIC** Wind power uncertainty incremental cost

April. 28, 2016. This work was supported by the China Scholarship Council (CSC) and technical project from China State Grid.

- J. Yan is with the State Key Laboratory of Alternate Electrical Power System with Renewable Energy Sources, School of Renewable Energy, North China Electric Power University, Beijing, China. She is doing a joint PhD at University of Bath, UK. (e-mail: yanjie_freda@163.com)
- Y.Q. Liu is with the State Key Laboratory of Alternate Electrical Power System with Renewable Energy Sources, School of Renewable Energy, North China Electric Power University, Beijing, China. (yqliu@ncepu.edu.cn)
- F. Li, and C. Gu are with Department of Electronic & Electrical Engineering, University of Bath, UK.

WPUDC

Wind power uncertainty dispatching cost

II. INTRODUCTION

IND power is increasingly contributing to the electricity supply worldwide because of its low environmental impact and negligible generation costsError! Reference source not found.. Limited predictability of intermittent wind generation creates uncertainty for system operation and market trading, which are based on the quality of wind power forecasting (WPF). However, balancing the load and generation for systems with large share of wind power could be technically and economically challenging. Specifically, larger spinning reserves are required to balance the possible deviations of wind power generation from forecasts. Frequent cycling of the operational thermal generators for balancing increases the outage and operational expenses. This balancing act increases the operation costs of the power system and reduces the value of wind power [1,2]. For operational planning in a renewable-rich power system, it is important to provide an accurate and efficient cost model in dealing with the situation-dependent uncertainty of wind power and investigate how such uncertainty affects system operation costs.

Previous studies have estimated the balancing cost incurred from wind power uncertainties, most achieved by directly comparing the total power system costs with uncertainties and fully predictable wind power [3,4,5,6]. However, such analysis is limited to payment mechanisms and unfit for the trading or operating decisions. Another set of approaches use historical probabilistic density function (PDF) of the wind speed or WPF deviation to establish the expected value of underestimation (reserve) costs and overestimation (curtailment) costs in a probabilistic and integral form. Some of them assumed wind speed PDF, such as Weibull distribution [7,8,9], and then transfer it to wind power PDF by using theoretical or mapping power curve of wind turbines [10]. Another group of approaches assume PDF of historical WPF deviations to obey given empirical distributions [11,12,13], such as Gaussian [14,15], Beta [16], etc. These methods are partly able to simulate the random distribution of wind power variable and balancing costs, but still leave several problems to be solved.

The use of historical distribution of WPF deviation implies that the uncertainty of wind power and its development cannot be evaluated at a particular time slot. In addition, the empirical PDF is proved to be unable to simulate the actual distribution. These two problems will, therefore, bring large errors in the cost calculation, and thus primarily require an accurate model for estimating the future uncertainties of wind power. Relevant

studies basically have two categories [17]. One category considers a range of possible real-world wind power output scenarios by using Monte Carlo or Markov simulations [18,19,20], etc. Scenario based methods generate a number of scenarios according to historical data and use scenario reduction techniques to select the representative scenarios and delete redundant ones. The difficulty here is how to choose the number of reduced scenarios because a large number of simulations can exponentially increase computing burden but a small number can result in poor approximation [21]. Another category is based on probabilistic forecasting, which generates a series of uncertain intervals under given confidence probabilities based on a per look-ahead time basis, for example, quantile regression [22] and relevance vector machine (RVM) [23,24]. They do not inform forecasting errors at a given prediction time point since they neglect the interdependence structure of forecast errors among look-ahead time [25]. This will bring successional risk to many time-dependent decision-making processes.

The inverse function of such mentioned cost models does not have an analytical form and thus makes system dispatch hard to be solved by traditional optimization algorithms but solved by artificial intelligent algorithms (such as PSO, etc.). This fact implies that the system operation method in a conventional system requires large changes or requires more computational burden in order to accommodate increasing wind generation.

In response to above problems, the main contribution of this paper is to introduce the concept of wind power uncertainty incremental cost (WPUIC) and wind power uncertainty dispatch cost (WPUDC) to enable wind power uncertainty cost in system operation. WPUIC is able to analytically present the incremental cost of accommodating uncertain wind power. WPUDC is developed to quantify the potential balancing cost associated with wind power uncertainties. Different from existing studies, the two models: i) they have an analytical form, which facilitates the system operation of a renewable power system easily; ii)they are able to differentiate the seasonal impacts and other external conditions by adjusting the characteristic parameters in the cost formulation. Continuous updates of the two parameters can benefit a rolling plan to instantaneously capture wind power uncertainties.

Moreover, this paper also proposes a wind power probabilistic forecasting (WPPF) model based on varying variance relevance vector machine (VVRVM) in order to estimate future uncertainties of wind power. Another contribution of the paper is that VVRVM is able to adjust the estimated uncertainty in each training iteration according to previous training deviation and current forecast level. Such varying variance adjusted with the error interdependence and variable weather conditions can facilitate more accurate uncertainty estimation at a given time point.

The rest of paper is organized as follows. Section III introduces a probabilistic forecasting method based on VVRVM to model the WPF uncertainty in cost formulation. Section IV describes the concept and formulation of WPUIC and WPUDC. A case study in Section VI investigates the WPF

uncertainty features and validates the proposed cost models. Finally, Section VII concludes the findings.

III. FORECASTING UNCERTAINTY FORMULATION

System operators and wind power producers are all subject to additional costs for balancing fluctuating wind generation. An accurate WPF model and uncertainty estimation can lay the foundation for advanced decision making in power system operation or market participation.

This section first proposes one probabilistic forecasting method based on VVRVM and demonstrates its results. The results of VVRVM are used as an example to demonstrate how a probabilistic forecasting method can serve for the proposed balancing cost modelling. Before the cost modelling, the probability with respect to given uncertain wind power range and the risk of failing to meet the wind power obligation are calculated based on the results of WPPF.

A. Probabilistic forecasting based on VVRVM

Given a set of input-target pairs $\{x_n, t_n\}_{n=1}^N$, assume that $t_i = y(x_i; w) + \varepsilon_i$. ε_i is Gaussian noise with mean zero and variance σ^2 . The prediction is made by

$$y(x; w) = w^{T} \varphi(x) = \sum_{i=1}^{M} w_{i} K(x, x_{i}) + w_{0}$$
 (1)

where, $\varphi(x)$ is the vector of a basis function; $w = (w_0, w_1, w_2, ..., w_M)$ is weights vector; $K(x, x_i)$ is kernel function; M is the total sample number.

Constraint on weights w_i was imposed by 'prior' probability distribution as below

$$p(w \mid \alpha) = \prod_{i=0}^{N} N(w_i \mid 0, \alpha_i^{-1})$$
 (2)

where, α is N+1 vector termed as 'hyperparameters'.

The posterior probabilities over unknown samples could be obtained from Bayesian inference. The learning process aims to search α, σ^2 ($\beta = \sigma^{-2}$) by using maximum marginal likelihood estimation. α, σ^2 are assumed to follow Gamma distributions with parameters of c,d, which affect the interval of the proposed forecasting uncertainty. They are variable with forecasting errors from last iteration and current inputs (including weather inputs and forecasts level). In this way, VVRVM is able to track real-time uncertainties and error interdependency in a more accurate manner.

The partial differential of the maximum likelihood function, which is shown in (3), is set to zero with respect to α and β . The results are shown in (4)-(7) [26].

$$L = -\frac{1}{2} \left[\log \left| \beta^{-1} \mathbf{I} + \varphi \mathbf{A}^{-1} \varphi^{T} \right| + t^{T} \left(\beta^{-1} \mathbf{I} + \varphi \mathbf{A}^{-1} \varphi^{T} \right)^{-1} t \right] + \dots$$

$$\dots + \sum_{i=0}^{N} c \log \beta - d\beta$$
(3)

$$\alpha_i^{\text{new}} = \frac{1 - \alpha_i \sum_{ii}}{\mu_i^2} \tag{4}$$

$$\left(\sigma^{2}\right)^{new} = \frac{\left\|t - \varphi\mu\right\|^{2} + 2d}{M - \Sigma_{i}\gamma_{i} + 2c}$$
 (5)

$$\mu = \sigma^{-2} \sum \varphi^{T} t \tag{6}$$

$$\sum = \left(\sigma^{-2} \sum \varphi^T t + A\right)^{-1} \tag{7}$$

where, μ_i is the i-th mean of the posterior from (6); \sum_{ii} is the i-th diagonal element of posterior covariance from (7), computed by α, σ^2 from current iteration. The superscript "new" means that the two parameters are newly updated value in the latest iteration, and they are updated in each iteration until convergence.

Assuming the new input to be x_* , the predicted distribution of wind power is as below [26].

$$y_* = \mu^T \varphi(x_*) \tag{8}$$

$$\sigma_*^2 = \sigma_{\text{MP}}^2 + \varphi(x_*)^T \sum \varphi(x_*) \tag{9}$$

where, y_* is the point forecasts; the subscript "MP" means "make prediction", which declares that the parameter is obtained from the final iteration and used to make a prediction. Details on RVM theory and RVM-based WPPF methods can be found in our prior work [23,24].

The results of VVRVM on a random day in December are shown in Fig.1. This case is based on a Chinese wind farm, whose details are given in the case study. Forecasting intervals under 90%, 80%, 70% and 60% confidence levels are drawn along with the deterministic power forecasts and actual power output. The reliabilities of all confidence levels are 93.1%, 82.3%, 70.7%, 61.6% respectively. Most estimated intervals are able to cover the fluctuations of actual power output by reasonable bounds, illustrating the reliability and sharpness of the VVRVM model.

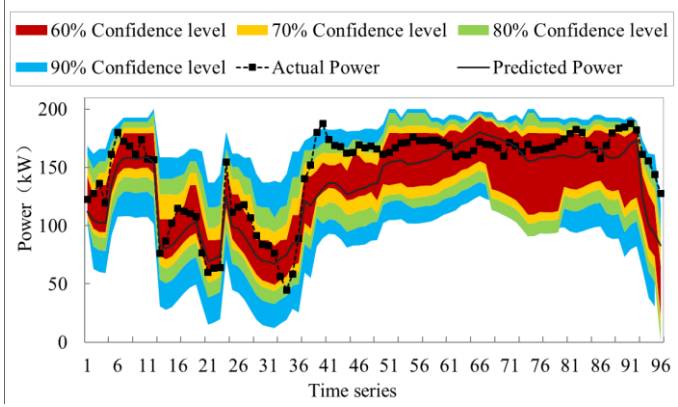


Fig.1 Probabilistic forecasting of VVRVM on a day in December

B. Probability of Uncertain Wind Power Range

Probabilistic forecasting, i.e. in the form of predictive distribution, basically has two aspects: uncertain range and probabilities. To capture the features, the probability with respect to given uncertain wind power range is calculated based on the VVRVM forecasts.

Considering a random wind power variable w, $f^{w}(.)$ represents its PDF and F(.) is its cumulative distribution

function (CDF). Given a wind power value x, the CDF of w can be expressed as

$$F(x) = \operatorname{Prob}(w \le x) = m \tag{11}$$

Quantile function $Q(m|w \le x)$, or written as Q(m), is the

inverse function of F(x) at confidence level τ ($\tau \in [0,1]$).

$$Q(m|w \le x) = F^{-1}(m) \tag{12}$$

According to above quantile definition, the forecasting interval generated from the probabilistic forecasting can be transformed to quantile version

$$I(\tau) = \lceil Q(m_l), Q(m_u) \rceil \tag{13}$$

where, τ is the theoretical confidence probability, at which the actual power production is within the given uncertain power range; $I(\tau)$ is forecasting interval; $Q(m_u)$ and $Q(m_l)$ are the upper and lower limits of future wind power respectively.

According to the definition of confidence level in quantile, m_u and m_l can be further inferred as follow.

$$m_u + m_l = 1 \tag{14}$$

$$m_u - m_l = \tau \tag{15}$$

$$m_u = \frac{1+\tau}{2}; \quad m_l = \frac{1-\tau}{2}$$
 (16)

With given predicted wind power (w^{pred}), the confidence probabilities of each uncertain power range ($\Delta = \left| w - w^{pred} \right|$) are calculated based on 24-hour ahead and 4-hour ahead WPPF. Fig.2 depicts the CDF of Δ . It is clear to see that three curves are monotonic decreasing and smaller forecasting horizon has a higher confidence level with the same uncertain power range. For the 24-hour ahead and 4-hour ahead forecasting, their confidence probability curves are approximately linear. As for the 1-hour ahead forecasting, it might need piecewise linearization. To sum up, CDF of Δ for each horizon can be linearized or piecewise linearized as below.

$$F(\Delta | w^{pred}) = a_1 \times \Delta + b_1 = \begin{cases} a_{11} \times \Delta^+ + b_{11}, \Delta^+ > 0 \\ a_{12} \times \Delta^- + b_{12}, \Delta^- < 0 \end{cases}$$
(17)

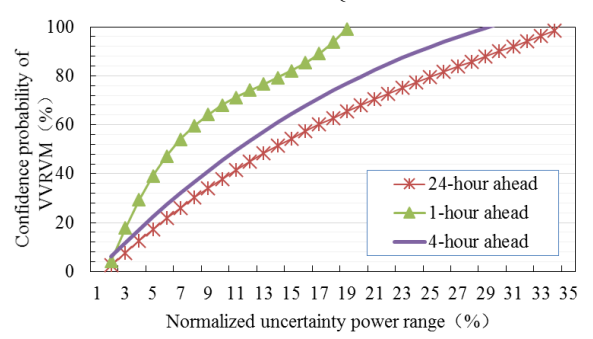


Fig.2 Confidence probability of VVRVM within each power range for different forecasting horizon

A series of $I(\tau)$ and m_u, m_l can be obtained by using VVRVM based WPPF and (13). The probabilities of a random wind power variable to be within a given range $[P_1, P_2]$ can be calculated by (18) based on CDF of Δ in (17).

$$\operatorname{Prob}(P_{1} < P \leq P_{2}) = F(P_{2}) - F(P_{1})$$

$$= F(Q(m_{2}|P_{2})) - F(Q(m_{1}|P_{1})) \qquad (18)$$

$$= m_{2} - m_{1}$$

Fig.3 depicts the relations between each given power range and its corresponding probability $\operatorname{Prob}(P_1 < P \le P_2)$. It can be seen that the probability curves for the 4-hour ahead and 24-hour ahead forecastings are stable at around 3%-6%. This to some extent validates the scientificity of (17). Meanwhile, the 1-hour ahead curve is close to a linear line initially but drops sharply from 14% to 0%. Thus, this linear relation can be written as below.

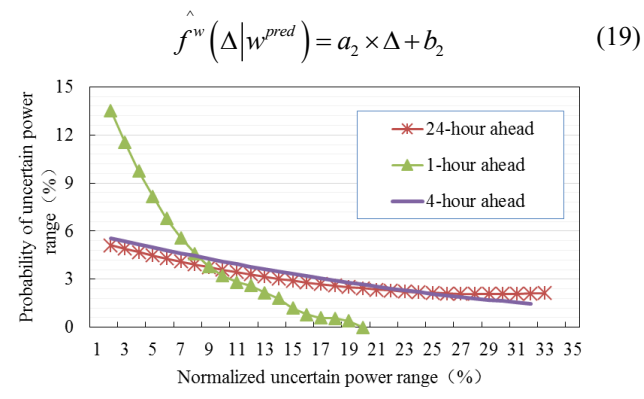


Fig. 3 Curves of the uncertain power range and its probability for different forecasting horizon

C. Risk Probability (RP) Function

Risk probability (RP) is proposed to quantify the probability of failure to meet the scheduled obligation. CDF of the uncertain power range Δ in (17) is used to derive the RP function

$$RP(w) = \begin{cases} 1 - Prob(\Delta^{-}) = 1 - Q_{w^{pred}}^{-1}(\tau) + Q_{w}^{-1}(\tau), & w^{pred} > w \\ 1 - Prob(\Delta^{+}) = 1 + Q_{w^{pred}}^{-1}(\tau) - Q_{w}^{-1}(\tau), & w^{pred} < w \end{cases}$$
(20)

where
$$\Delta^+ = w - w^{pred}$$
; $\Delta^- = w^{pred} - w$.

According to (17), the relationship between uncertain power range and its corresponding risk probability can be written as a linear function with respect to dual characteristic parameters in (21). Two characteristic parameters in the RP function are termed as *scale parameter* and *margin parameter*, which vary with weather conditions or specific wind farms. Adjustable parameters allow RP function to reflect the seasonality and dispersion of stochastic wind.

$$RP(w) = c_{RP} \left| w - w^{pred} \right| + b_{RP}$$
 (21)

where, b_{RP} is the interception of RP function, termed as "scale parameter", indicating the average magnitude of the WPF deviation; c_{RP} is the slope of RP function or marginal risk, termed as "margin parameter", indicating the dispersion of the WPF error distribution. A small marginal risk reflects a fairly stable WPF performance probably due to a simple meteorological pattern.

This RP function is used to analyze and validate the following proposed WPUDC model. The so-called "risk" relates to two issues: i) the fast start-up and more reserves for

the deficiencies of wind power, and ii) the curtailment for overscheduling wind power.

IV. UNCERTAINTY COST FORMULATION

A. Concept and formulation of WPUIC

The incremental cost of power production in a power system, whatever from renewables or conventional generators, is a basic way to expose the mechanism of economic dispatching and market clearing [27]. The incremental cost of a conventional generator varies depending on load level, machine type and fuel price, which is relatively easy to formulate. Renewables have nearly zero incremental fuel cost, but the balancing costs for wind power can be substantially high because of errors in hour-by-hour forecasting [28].

Much of up-to-date research has concentrated on the use of a total cost model by system operators. However, they are not able to discriminate between wind power producers who incur additional balancing costs or auxiliary service reinforcement, and those who reduce the system imbalance. It is for this reason that the concept of WPUIC and WPUDC are introduced to quantify the additional cost for balancing uncertain wind power in a power system.

In this section, wind power uncertainty incremental cost (WPUIC) is defined to quantify the extra balancing cost for increasing unit wind power generation in a power system. The definition of WPUIC is as below.

WPUIC
$$(P_w) = \frac{\partial E[Cost_{imb}(\Delta P_{imb})]}{\partial P_w}$$
 (22)

where, P_w is the scheduled wind power generation; $\Delta P_{imb} = |w^{act} - P_w|$ is the power deviation between scheduled wind power and actual generation; $\operatorname{Cost}_{imb}\left(\Delta P_{imb}\right)$ is the cost for balancing power deviation from wind in the future; $\operatorname{E}\left[\operatorname{Cost}_{imb}\left(\Delta P_{imb}\right)\right]$ is the mathematical expectation of $\operatorname{Cost}_{imb}\left(\Delta P_{imb}\right)$.

For power and energy balance in a system, if a wind power producer has underproduction or overproduction compared to the contracted amount due to the partial predictability of wind, the energy difference must be settled by energy imbalance price (EIP) as unit payments. Specifically, it must purchase the shortfall at System Sell Price (SSP) or sell the surplus at System Buy Price (SBP) [29]. These prices can help to quantify the costs to balance wind energy deviations.

The balancing cost and its mathematical expectation are defined as

$$\operatorname{Cost}_{imb}(P_{w}) = \begin{cases} C_{p}(P_{w}) = k_{p} | w^{act} - P_{w} |, w^{act} - P_{w} > 0 \\ C_{r}(P_{w}) = k_{r} | P_{w} - w^{act} |, w^{act} - P_{w} < 0 \end{cases}$$
(23)

$$E\left[\operatorname{Cost}_{imb}\left(P_{w}\right)\right]$$

$$=\int_{Q(m_{t})}^{Q(m_{u})} \operatorname{Cost}_{imb}\left(P_{w}\right) g\left(x\right) dx \qquad (24)$$

$$=k_{r} \int_{Q(m_{t})}^{P_{w}} \left(P_{w}-x\right) g\left(x\right) dx + k_{p} \int_{P}^{Q(m_{u})} \left(x-P_{w}\right) g\left(x\right) dx$$

where, k_p , k_r are the unit price for the curtailment at SSP and the reserve at SBP respectively; g(x) is the predicted PDF of future wind power variable; $C_p(P_w)$ is the costs for balancing the overproduction of wind; $C_r(P_w)$ is the costs for balancing the underproduction of wind; $Q(m_u)$, $Q(m_l)$ is the upper and lower limits of each forecasting interval respectively, which can be set to [0,1] (normalized power value) as a conservative range.

Therefore, WPUIC can be formulated as

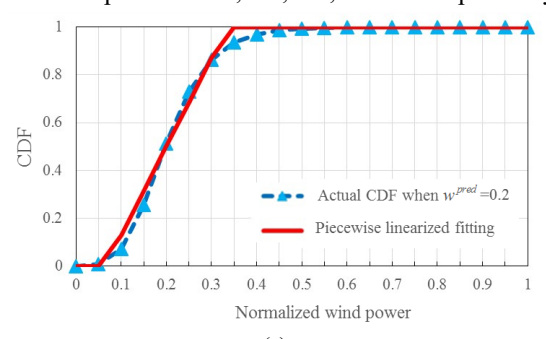
WPUIC =
$$\frac{\partial E\left[\operatorname{Cost}_{imb}\left(P_{w}\right)\right]}{\partial P_{w}}$$

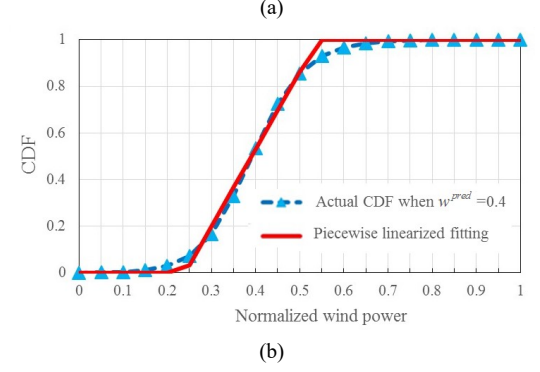
$$= \frac{\partial E\left[C_{p}\left(P_{w}\right)\right]}{\partial P_{w}} + \frac{\partial E\left[C_{r}\left(P_{w}\right)\right]}{\partial P_{w}}$$

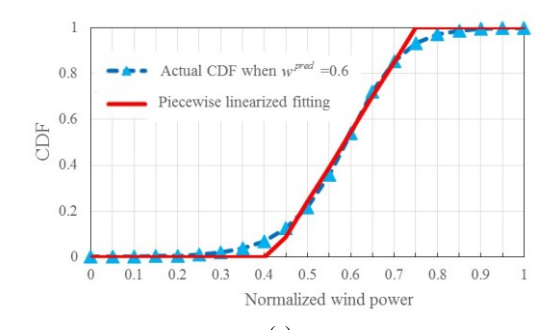
$$= k_{r}G\left(P_{w}\right) - k_{r}G\left(Q\left(m_{u}\right)\right) - k_{p}G\left(Q\left(m_{l}\right)\right) + k_{p}G\left(P_{w}\right)$$
(25)

where, G(.) is the predicted CDF of future wind power variable generated from a WPPF method and in this paper it is VVRVM.

In this case, the predicted CDF of wind power variable χ is piecewise linear functions with three segments. Fig.4 show the predicted CDF curves with different normalized WPF value. The red curve is the proposed and linearized piecewise CDFs of future wind power, while the blue one is the non-linearized raw CDF. The average absolute deviations between the two curves are 1.91%, 1.58%, 2.37%, and 1.55%, when the normalized predicted wind power is 0.2, 0.4, 0.6, and 0.8 respectively.







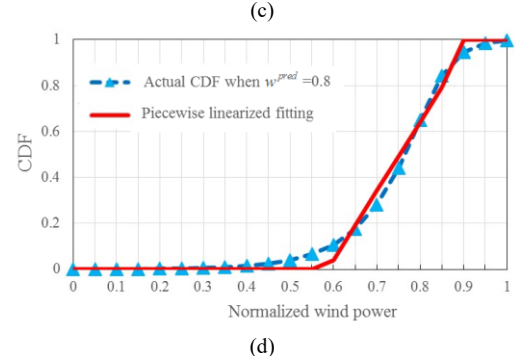


Fig. 4 Curves of the actual CDF and the piecewise linearized predictive CDF

From Fig.4, the predictive CDF can be written as a piecewise function with three segments in (26). Further, the predictive PDF can be written as (17)

$$G(x) = \begin{cases} 0, & 0 \le x < -b/a \\ ax + b, & -b/a \le x < (1-b)/a \\ 1, & (1-b)/a \le x \le 1 \end{cases}$$
 (26)

$$g(x) = \begin{cases} 0, & 0 \le x < -b/a \\ a, & -b/a \le x < (1-b)/a \\ 0, & (1-b)/a \le x < 1 \end{cases}$$
 (27)

Integrating (26) into (25), WPUIC can be rewritten as a piecewise function, which consists of a linear function with respect to P_w and a constant. The detailed process to calculate the WPUIC can be found in Appendix A.

$$WPUIC(P_w) = \begin{cases} C \\ M \cdot P_w + N \end{cases}$$
 (28)

where, C, M, N are constant depending on values of k_p, k_r, P_w , and $Q(m_u), Q(m_l)$.

B. Formulation of WPUDC

This section defines wind power uncertainty dispatch cost (WPUDC) as the mathematical expectation of the operational costs for balancing deficits or surplus incurred by WPF uncertainties.

According to Newton-Leibniz theorem, WPUDC function can be rewritten in (29), where *Const* is a constant.

WPUDC
$$(P_w) = E[Cost_{imb}(P_w)]$$

= $\int_{0}^{P_w} WPUIC(w)dw + Const$ (29)

To validate the mathematical scientificity of the proposed

modelling, we deduce WPUDC function from both CDF and PDF perspectives as cross-validation. In the CDF deducing method, the predictive CDF with respect to uncertain power range is firstly used to calculate WPUIC, and then it is integrated into (29) to calculate WPUDC. In the PDF deducing method, the predictive PDF is used instead to be integrated into (24). The details of the deducing processes and resultant WPUDC function can be found in the Appendix B. The resultant WPUDC is a piecewise function with three segments, whose second segment is shown as a quadratic function

$$WPUDC(P_w) = \alpha_w P_w^2 + \beta_w P_w + \gamma_w$$
 (30)

where, α_w , β_w , γ_w are adjustable parameters in WPUDC.

To examine the impacts of curve linearization on the model precision, the results of CDF deducing and PDF deducing methods are compared to the actual integral results without linearization in Fig.5. It is seen that the results from the two deducing techniques match very well with the actual integral results. In addition, their average absolute deviations are 1.31 and 1.13 in cost unit.

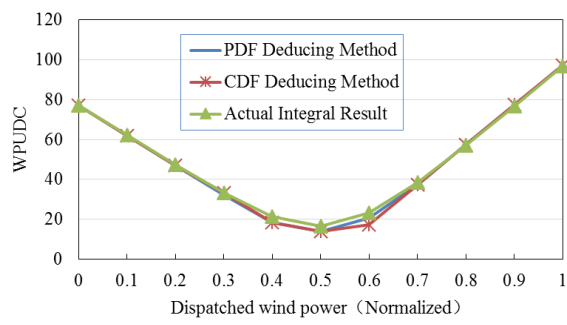


Fig. 5 Results of two deducing methods and the actual integral

This section emphasizes the definition and modelling of WPUDC and EIP (k_p, k_r) is assumed to be constant. In above figure, the parameters are set to $w^{pred} = 0.45$, $k_p = 150$, $k_r = 200$.

C. Properties of WPUDC Model

Two valuable properties of the proposed cost model are:

- 1) WPUDC can better quantify the features of forecasting uncertainties with respect to any meteorological conditions and forecasted power magnitude, by adjusting parameters to suitable values. The generality of WPUDC is attributed to the adjustable scale and margin parameters. This allows WPUDC to facilitate rolling scheduling.
- 2) It is a convex problem which can be easily incorporated in a typical optimization problem, such as system dispatching. This minimizes the effort to transform system dispatching for a traditional high-carbon system to a low-carbon system and also increases system efficiency with more penetration of uncertain renewable.

D. Discussion

Firstly, each wind power producer is assumed to be a price taker and does not affect market prices for energy or ancillary services. k_p, k_r are assumed to be asymmetric and constant in the case study, because the proposed cost is mainly about

incorporating situation-dependent wind power uncertainty into balancing cost, which is important for power system operation with large wind power penetration. The proposed cost model is built to reveal the features of actual forecasting uncertainty and its influence on risk probability proved in Fig.9-10. The results will not be affected by the price assumption. Besides, many previous works have assumed constant prices [7,21,30], and thus we think that the conclusion and contribution will not be compromised if the prices are assumed to be constant. To supplement the results with the assumed constant prices, several price pairs of k_n, k_r are selected according to the daily average prices in December of 2015 in the UK [29] to demonstrate the impact changing prices on balancing cost. This new effort can represent the actual daily average status of prices to some extent since both extreme situations and average situations are included. In the case study, the prices are set equal to their average values; or/and another ranges from the minimum to maximum. Our future work will be dedicating to modelling these parameters.

Secondly, we use a piecewise function to approximate the CDF of wind power to formulate WPUDC. In this case, the results in Fig.4 and Fig.5 proved that three segments can be well fitting the actual CDF. If more accurate results are desirable, more segments should be used.

V. CASE STUDY

A. Data

This case study considers the operation data from a wind farm in North China, containing actual wind power generation as well as numerical weather prediction (NWP) in 2010. Based on these data, the developed VVRVM based probabilistic forecasting model is established. The forecasting horizon is 24 hours and the time resolution is 15 minutes. The installed capacity of this wind farm is 183 MW.

The normalized value of power is calculated by dividing wind farm installed capacity in order to facilitate future comparison with other wind farms. WPF deviation is given by the predicted power minus actual wind power.

B. Features of Forecasting Uncertainties

Based on the features of WPF uncertainties, the proposed RP function and cost models can be validated accordingly. Results show that WPF uncertainties have two main features with respect to the forecasted magnitude and season.

1) Uncertainties for Given Forecasted Magnitude

Results in Fig.6 and Fig.7 show that: i) The absolute forecasting deviation increases with the growth of power output in every season. ii) For a small power output, the probability distribution is concentrated or "pointed" and the forecasted value tends to be closer to the actual value. iii) For a large power output, the probability distribution is dispersive or "flat" and the forecasted value tends to be dispersed from the actual value.

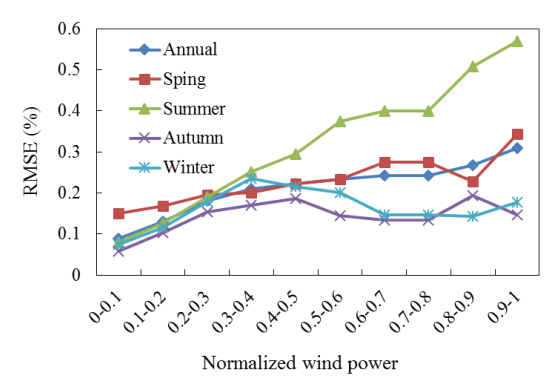


Fig.6 Deviation interval for given normalized wind power output in different seasons

Fig.7 provides the probability distribution of the forecasting deviation for various forecasted power output. The distribution shapes are not symmetrical. For example, for 0-0.1 normalized forecasted wind power in the front row, the highest probability bar is up to 50%, and the corresponding normalized WPF deviation is zero. The probabilities for negative deviation are nearly 45%, while the positive deviation is only less than 5%. For 0.91-1 normalized forecasted magnitude at the end of row (dark purple bar), the highest probability bar decreases to less than 40%, where the normalized WPF deviation is around 0.5 and 0.6. Probabilities for the negative deviations are less than 3%, while they increase to about 95% for the positive deviation.

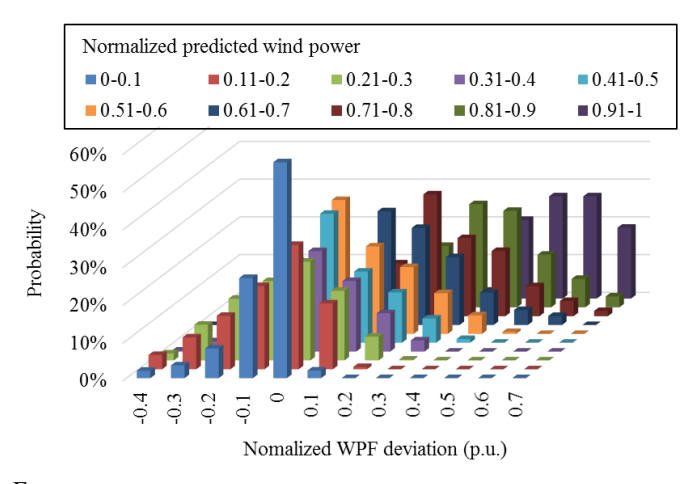


Fig. 7 Probabilistic distribution of WPF deviation for various normalized WPF magnitude

2) Uncertainties for Given Season

With changing weather system, the magnitude and distribution of WPF deviation change accordingly. Results in Fig. 8 show that: i) during winter, the meteorological pattern is relatively simple and easy to simulate. Hence, NWP and WPF are more accurate. ii) During summer, WPF's RMSE is normally low because of wind scarcity. iii) During spring and autumn, WPF's RMSE increases. This is because that the meteorological condition is unstable and complex and thus wind fluctuates frequently and dramatically. Under this circumstances, the mechanical failures could make WPF be more difficult.

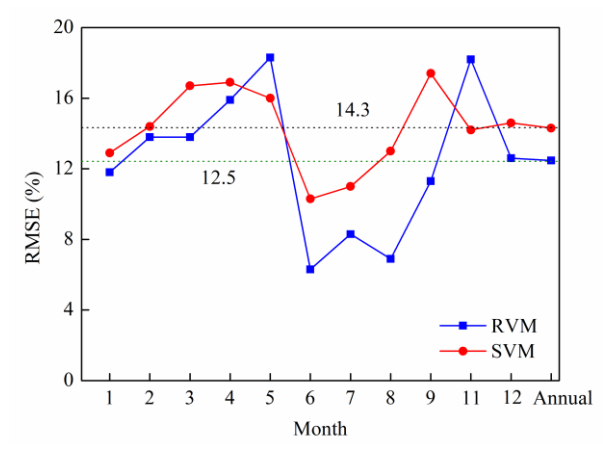


Fig. 8 Monthly RMSE from support vector machine (SVM) and VVRVM WPF models

C. Results for Risk Probability (RP)

In Fig.9, the RP curves show consistent features of WPF uncertainty. Firstly, the probability of not meeting the contracted obligation in every season generally tends to increase with the growth of uncertain wind power range. Secondly, spring generally has the highest risk of not meeting the contracted obligation; autumn takes the second place; winter is the third, and summer is the smallest. This trend is consistent to that of monthly WPF's RMSE. Summer has the sharpest slope, followed by spring, autumn, and winter. Specifically, the lowest point of the RP curve appears at the beginning, while the highest appears at the end of the summer's curve. This is because that summer has comparatively accurate WPF, especially when the generated power level is low. But, it is risky to schedule a large wind power commitment considering the scarce wind availability during summer. Winter has a small slope of the RP curve, reflecting "flat" probability distribution of WPF deviation, especially for a relatively large wind power magnitude. The intercept of RP curve represents the average magnitude of uncertainty, while the slope of the RP curve represents the shape of the probability distribution of WPF deviation.

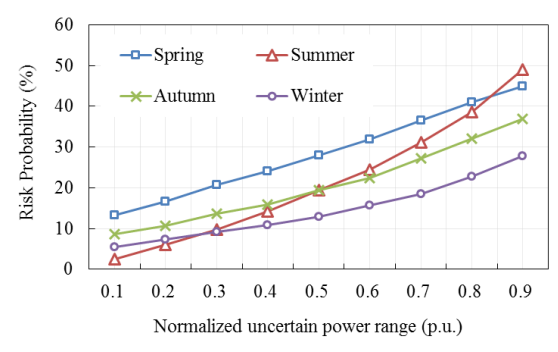


Fig. 9 Risk probability with respect to absolute value of uncertain wind power range in each season

Fig.10 is the RP curves with respect to each wind power uncertain range. These curves are all parabola and have one lowest point with minimum risk probability, which refers to the safest scheduling point. Traditionally, system operators make dispatch the system based on the deterministic WPF without any uncertainty description, which is represented by the point

of "0" uncertain wind power range on the X-axis. However, the safest scheduling point is not at "0" uncertain power range in this figure. This illustrates that the deterministic forecasting definitely brings risks in dispatching.

Besides, the lowest RP points on different curves locate at various positions of X-axis, i.e. various normalized uncertain wind power range. For a small forecasted wind power, the safest point is on the positive side of the X-axis (positive uncertain power range), reflecting that the underestimation is more likely to appear for WPF. For large forecasted power, the overestimation is more likely to happen, and thus the safest scheduling point is on the negative side of the X-axis (negative uncertain power range). In Fig.10, the safest points for 0.1-0.5 normalized wind power are on the positive side, while the safest points for 0.51-1 magnitude are on the negative side. Specifically, the safest scheduling point locates at around 0.2 and -0.4 uncertain power range for 0-0.1 and 0.9-1 normalized forecasted wind power, respectively.

Lastly, a smaller magnitude of forecasted power has smaller risk probability, which is also consistent with the features of WPF uncertainty. The dark blue curve representing 0-0.1 normalized wind power generation has the lowest risk.

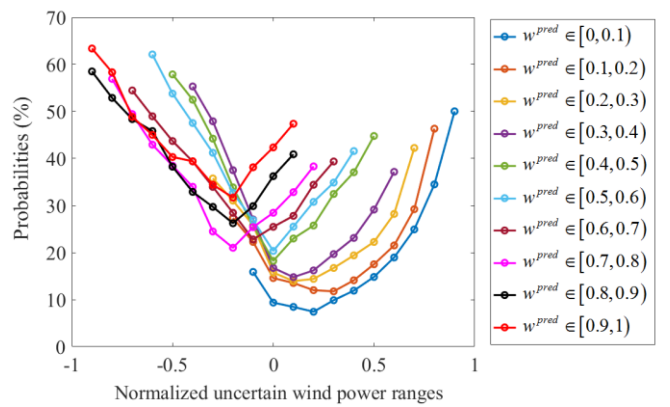


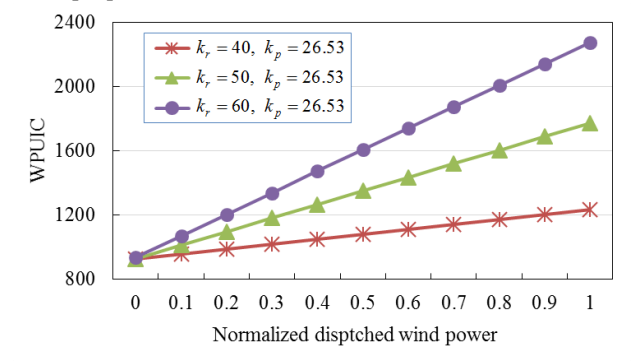
Fig. 10 RP curves with respect to normalized uncertain wind power ranges

Thus, if a system operator makes an inflexible schedule following deterministic WPF, there could be dual unfavorable situations: i)one is the waste of unexpected wind energy when WPF deviation is negative; ii)another is to bear more risk and high operational costs for the rapid start-up and for balancing wind power deficits. Therefore, with the assistance of these RP curves, system operators can estimate the differential of balancing cost with respect to scheduled wind power. They can adjust the original WPF to power commitment with the lowest risk on the RP curves.

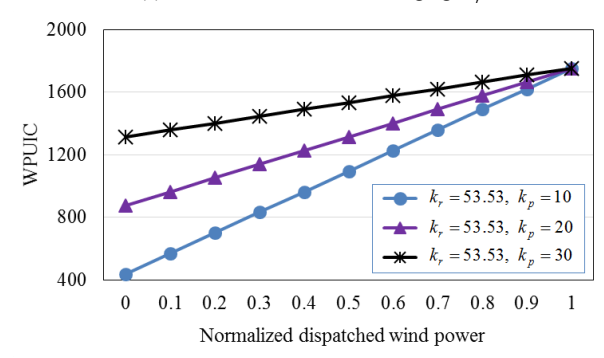
D. Results for cost calculations

In Fig.11, WPUIC increases with growing scheduled wind power, which indicates that the impacts of wind power uncertainty on balancing cost are linearly aggravating with the increase. Especially with higher EIP, the impacts are more sensitive, which is reflected in this figure that the curve slope is very sharper with higher EIP. A Larger share of wind power in a power system needs more auxiliary services and the cost for balancing per unit increase gradually. It is noted that these prices are selected according to the actual prices in the UK [29].

The monthly average prices are $k_p = 26.53$, $k_r = 53.53$. Fig.12 is the daily average system price over in December of 2015 in the UK [29].



(a) Curves of WPUIC with changing k_r



(b) Curves of WPUIC with changing k_n

Fig. 11 Curves of WPUIC and dispatched wind power with different EIP

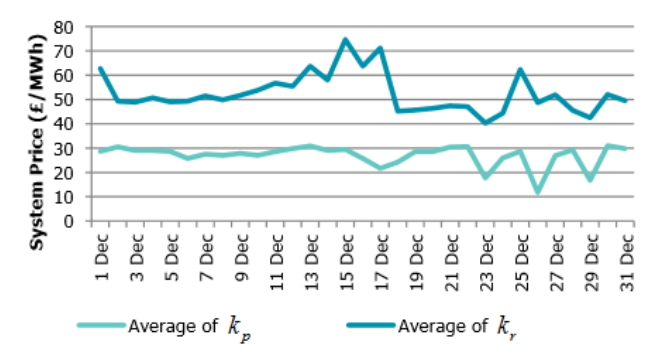


Fig. 12 Daily average system price over the Dec. of 2015 in the UK

Fig.13 depicts the relations between WPUDC and the scheduled wind power under different WPF values. Parameters are set to $k_p = 26.53$, $k_r = 53.53$. WPUDC reaches its lowest point at around WPF value, which indicates the significance of WPF technologies and the deficiency of deterministic forecasting. The lowest cost does not appear if the operator dispatches wind power according to deterministic forecasting value. For example, when $w^{pred} = 0.1$, the lowest cost appears when the dispatched wind power is around 0.22; if $w^{pred} = 0.5$, the lowest cost appears when the dispatched wind power is around 0.39; when $w^{pred} = 0.9$, the lowest cost appears if the dispatched wind power is around 0.75. This illustrates the necessity of the probabilistic forecasting and uncertainty modelling.

Besides, the scheduled wind power with the minimum cost locates below the predicted wind power value when the predicted value is high. On the contrary, when the predicted wind power is low, the scheduled wind power with the minimum cost locates above the predicted value. Meanwhile, when future wind power is predicted to be high, the lowest cost point locates further away from the predicted value than that with lower wind penetration. This phenomenon is consistent to the features of WPF deviation and thus can serve system scheduling to minimize balancing cost and risk.

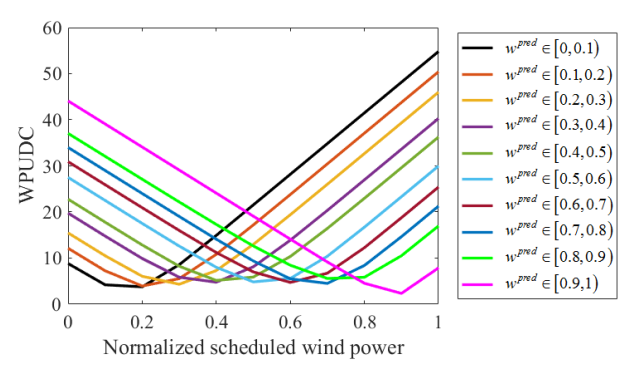


Fig. 13 Curves of WPUDC and dispatched wind power with different predicted wind power

VI. CONCLUSION

This paper defines WPUIC and WPUDC to quantify the impacts of wind power uncertainty on the additional costs from balancing WPF deviations. Formulations of WPUIC and WPUDC are presented based on a newly developed probabilistic forecasting model, VVRVM, for better estimating WPF uncertainties. Through demonstration, the following conclusions are reached:

- Unlike a fixed cost function for all external conditions, WPUIC and WPUDC consider the seasonal diversities by adjusting two characteristic parameters. This improves model accuracy and enables flexible scheduling of wind power considering the distribution of situation-dependent future uncertainties.
- WPUDC has an analytic form having a quadratic function, which can improve grid's operational efficiency with increasing renewable penetration. In addition, the results reveal the impact of forecasting uncertainties on the risk probability and cost variations.
- RP function is established to quantify the probability of failing to meet power obligations. It has consistent features to WPF uncertainties with respect to power magnitude and season. It can also help to illustrate the essential mechanism of how deterministic forecasting induces risk and cost during dispatching.
- VVRVM model is proposed to predict deterministic results and future probabilistic uncertainty. Considering the interdependence of forecasts error and weather inputs, the predicted variance is recursive towards the deviation targets by adjusting hyper-parameter in raw RVM. In this way, better estimation of WPF uncertainties can be achieved for computing more accurate balancing costs.

VII. APPENDIX A

In this part, the WPUIC function can be derived in detail.

(1) When
$$-\frac{b}{a} < \frac{1-b}{a} < Q(m_u) < P_w < Q(m_l)$$
,
WPUIC $(P_w) = 0$

(2) When
$$-\frac{b}{a} < Q(m_u) < \frac{1-b}{a} < P_w < Q(m_l)$$
,
WPUIC $(P_w) = k_v (1 - a \cdot Q(m_u) - b)$

(3) When
$$-\frac{b}{a} < Q(m_u) < P_w < \frac{1-b}{a} < Q(m_l)$$
,
WPUIC $(P_w) = (k_n + k_r) \cdot (aP_w + b) - k_r (a \cdot Q(m_u) + b) - k_n$

(4) When
$$-\frac{b}{a} < Q(m_u) < P_w < Q(m_l) < \frac{1-b}{a}$$
,
WPUIC $(P_w) = (k_p + k_r) \cdot (aP_w + b) + \dots$
 $\dots - k_r (a \cdot Q(m_u) + b) - k_n (a \cdot Q(m_l) + b)$

(5) When
$$Q(m_u) < -\frac{b}{a} < P_w < Q(m_l) < \frac{1-b}{a}$$
,
WPUIC $(P_w) = (k_p + k_r) \cdot (aP_w + b) - k_p (a \cdot Q(m_l) + b)$

(6) When
$$Q(m_u) < P_w < -\frac{b}{a} < Q(m_l) < \frac{1-b}{a}$$
,
WPUIC $(P_w) = k_p (a \cdot Q(m_l) + b)$

(7) When
$$Q(m_u) < P_w < Q(m_l) < -\frac{b}{a} < \frac{1-b}{a}$$
, WPUIC $(P_w) = 0$

VIII. APPENDIX B

In this part, two deducing methods are used to cross-validate the formulation of WPUDC. And the comparison of two deducing methods to the real data is shown in Fig.5.

Assumed that W_j is the scheduled wind power in *j-th* wind farm or the *j-th* wind turbine; CDF of the future wind power variable x is G(x) as in (16), and its piecewise functions in three segments are $G_1(x), G_2(x), G_3(x)$ respectively; the predictive PDF is g(x) as shown in (27).

A. CDF Deducing Method

According to (29), WPUDC function at different wind power values is as below.

$$\begin{split} &\int_{0}^{w_{j}} G_{1}(x) dx + CC_{1}, \qquad 0 \leq x < -b/a \\ &\int_{0}^{-b/a} G_{1}(x) dx + \int_{-b/a}^{w_{j}} G_{2}(x) dx + CC_{2}, \qquad -b/a \leq x < (1-b)/a \\ &\int_{0}^{-b/a} G_{1}(x) dx + \int_{-b/a}^{(1-b)/a} G_{2}(x) dx + \int_{(1-b)/a}^{w_{j}} G_{3}(x) dx + CC_{3}, \qquad (1-b)/a \leq x < 1 \end{split}$$

(1) When
$$w_i \in [0, -b/a]$$
,

WPUDC₁
$$(w_j) = \int_0^{w_j} k_p [G_1(x) - 1] + k_p G_1(x) dx + CC_1$$

= $\int_0^{w_j} -k_p dx + CC_1$
= $-k_p w_j + CC_1$

(2) When
$$w_i \in [-b/a, (1-b)/a]$$
,

$$\begin{split} \text{WPUDC}_2 \Big(w_j \Big) &= \int_0^{-b/a} k_p \Big[G_1(x) - 1 \Big] + k_r G_1(x) dx + \int_{-b/a}^{w_j} k_p \Big[G_2(x) - 1 \Big] + k_r G_2(x) dx + CC_2 \\ &= \int_0^{-b/a} - k_p dx + \int_{-b/a}^{w_j} k_p \big[ax + b - 1 \big] + k_r \big[ax + b \big] dx + CC_2 \\ &= \frac{bk_p}{a} + \frac{a \big(k_p + k_r \big)}{2} w_j^2 + \Big[bk_r + \big(b - 1 \big) k_p \Big] w_j + \dots \\ &\dots - \left\{ \frac{b^2 \big(k_p + k_r \big)}{2a} - \frac{b \big[bk_r + \big(b - 1 \big) k_p \big]}{a} \right\} + CC_2 \end{split}$$

(3) When $w_i \in [(1-b)/a, 1)$,

$$\begin{split} \text{WPUDC}_{3}\left(w_{j}\right) &= \int_{0}^{-b/a} k_{p} \left[G_{1}\left(x\right) - 1\right] + k_{r} G_{1}\left(x\right) dx + \int_{-b/a}^{(1-b)/a} k_{p} \left[G_{2}\left(x\right) - 1\right] + \dots \\ & \dots + k_{r} G_{2}\left(x\right) dx + \int_{(1-b)/a}^{w_{j}} k_{p} \left[G_{3}\left(x\right) - 1\right] + k_{r} G_{3}\left(x\right) dx + CC_{3} \\ &= \int_{0}^{-b/a} - k_{p} dx + \int_{-b/a}^{(1-b)/a} k_{p} \left[ax + b - 1\right] + k_{r} \left[ax + b\right] dx + \int_{(1-b)/a}^{w_{j}} k_{r} dx + CC_{3} \\ &= \frac{bk_{p}}{a} + \frac{\left(k_{p} + k_{r}\right)\left(b - 1\right)^{2}}{2a} + \frac{\left(b - 1\right)\left[bk_{r} + \left(b - 1\right)k_{p}\right]}{a} + k_{r} \left(w_{j} + \frac{b - 1}{a}\right) + CC_{3} \end{split}$$

The values of each function at turning points are the same, because this piecewise function has no discontinuities. Knowing this, the constant items CC_1, CC_2, CC_3 in equation sets can be solved.

$$F_{1}\left(-\frac{b}{a}\right) = F_{2}\left(-\frac{b}{a}\right)$$
$$F_{2}\left(\frac{1-b}{a}\right) = F_{3}\left(\frac{1-b}{a}\right)$$

The solving result is $CC_1 = CC_2 = CC_3$.

B. PDF Deducing Method

Using PDF for the future wind power variable, WPUDC deducing process is as below.

(1) When
$$w_{j} \in [0, -b/a]$$
,
WPUDC₁ $(w_{j}) = C_{p}(w_{j}) + C_{r}(w_{j})$

$$= k_{p} \int_{w_{j}}^{1} (x - w_{j}) g(x) dx + k_{r} \int_{0}^{w_{j}} (w_{j} - x) g(x) dx$$

$$= k_{p} \left[\int_{w_{j}}^{-b/a} 0 \cdot (x - w_{j}) dx + \int_{-b/a}^{(1-b)/a} (x - w_{j}) (ax + b) dx + \int_{(1-b)/a}^{1} 0 \cdot (x - w_{j}) dx \right]$$

$$= k_{p} \left[\frac{a}{2} x^{2} - aw_{j} x \right]_{-b/a}^{(1-b)/a}$$

$$= k_{p} \left[\frac{(b-1)^{2}}{2a} + w_{j}(b-1) - \left(bw_{j} + \frac{b^{2}}{2a}\right) \right]$$

(2) When
$$w_i \in [-b/a, (1-b)/a)$$
,

$$\begin{aligned} \text{WPUDC}_{2}\left(w_{j}\right) &= C_{p2}\left(w_{j}\right) + C_{r2}\left(w_{j}\right) \\ &= k_{p} \int_{w_{j}}^{1} \left(x - w_{j}\right) g\left(x\right) dx + k_{r} \int_{0}^{w_{j}} \left(w_{j} - x\right) g\left(x\right) dx \\ &= k_{p} \left[\int_{w_{j}}^{(1-b)/a} a \cdot \left(x - w_{j}\right) dx + \int_{(1-b)/a}^{1} 0 \cdot \left(x - w_{j}\right) dx \right] + kr \left[\int_{-b/a}^{w_{j}} a\left(w_{j} - x\right) dx \right] \\ &= k_{p} \left[\frac{a}{2} x^{2} - aw_{j} x \right]_{w_{j}}^{\left(1-b\right)/a} + k_{r} \left(aw_{j} x - \frac{a}{2} x^{2} \right) \Big|_{-b/a}^{w_{j}} \\ &= k_{p} \left[\frac{(b-1)^{2}}{2a} + w_{j} \left(b - 1\right) - \frac{-aw_{j}^{2}}{2} \right] + k_{r} \left[\frac{aw_{j}^{2}}{2} + \left(bw_{j} + \frac{b^{2}}{2a} \right) \right] \end{aligned}$$

$$(3) \text{ When } w_{j} \in \left[\left(1 - b\right) / a, 1 \right),$$

$$\text{WPUDC}_{3}\left(w_{j}\right) = C_{p3}\left(w_{j}\right) + C_{r3}\left(w_{j}\right) \\ &= k_{p} \int_{w_{j}}^{1} \left(x - w_{j}\right) g\left(x\right) dx + k_{r} \int_{0}^{w_{j}} \left(w_{j} - x\right) g\left(x\right) dx \\ &= k_{r} \left[\int_{0}^{-b/a} 0 \cdot \left(w_{j} - x\right) dx + \int_{-b/a}^{(1-b)/a} a \cdot \left(w_{j} - x\right) dx + \int_{(1-b)/a}^{w_{j}} 0 \cdot \left(w_{j} - x\right) dx \right] \\ &= k_{r} \left(aw_{j} x - \frac{a}{2} x^{2} \right) \begin{vmatrix} (1 - b)/a \\ -b/a \end{vmatrix}$$

$$&= k_{r} \left[w_{j} - \frac{(b-1)^{2} + b^{2}}{2a} \right]$$

IX. REFERENCES

- [1] Y.V. Makarov, P.V. Etingov, Jian Ma, Zhenyu Huang, "Incorporating Uncertainty of Wind Power Generation Forecast Into Power System Operation, Dispatch, and Unit Commitment Procedures," Sustainable Energy, IEEE Transactions on, vol. 2, no. 4, pp. 433 442, 2011.
- [2] T. Aigner, S. Jaehnert, G.L. Doorman, T. Gjengedal, "The Effect of Large-Scale Wind Power on System Balancing in Northern Europe," Sustainable Energy, IEEE Transactions on, vol. 3, no. 4, pp. 751 - 759, 2012.
- [3] P. Meibom, C. Weber, R. Barth, H. Brand, "Operational costs induced by fluctuating wind power production in Germany and Scandinavia," *IET Renewable Power Generation*, vol. 3, no. 1, pp. 75 - 83, 2009.
- [4] E. Ela, M. O'Malley, "Studying the variability and uncertainty impacts of variable generation at multiple timescales," *IEEE Trans. Power Syst.*, vol. 27, no. 3, pp. 1324 - 1333, 2012.
- [5] A. Helander, H. Holttinen, J. Paatero, "Impact of wind power on the power system imbalances in Finland," *IET Renewable Power* Generation, vol. 4, no. 1, pp. 75 - 84, 2010.
- [6] M. Qadrdan, J. Z. Wu, N. Jenkins, and J. Ekanayake, "Operating strategies for a GB integrated gas and electricity network considering the uncertainty in wind power forecasts," *IEEE Trans. Sust. Energy*, vol. 5, pp. 128 - 138, Jan. 2014.
- [7] J. Hetzer, D. C. Yu, and K. Bhattarai, "An economic dispatch model incorporating wind power," *IEEE Trans. Energy Conversion*, vol.23, no.2, pp. 603 - 611, June 2008.
- [8] D. Villanueva, A. Feijóo, and J. L. Pazos, "Simulation of correlated wind speed data for economic dispatch evaluation," *IEEE Trans. Sust. Energy*, vol. 3, no. 1, pp. 142 - 149, Jan. 2012.
- [9] X. Liu and W. S. Xu, "Economic load dispatch constrained by wind power availability: A Here-and-Now approach," *IEEE Trans. Sust. Energy*, vol. 1, no. 1, pp. 2 - 9, April, 2010.
- [10] M. Moeini-Aghtaie, P. Dehghanian, M. Fotuhi-Firuzabad, and A. Abbaspour, "Multi agent Genetic Algorithm: An online probabilistic view on economic dispatch of energy hubs constrained by wind availability," *IEEE Trans. Sust. Energy*, vol. 5, no. 2, pp. 699 708. April, 2014.
- [11] F. Bouffard and F. D. Galiana, "Stochastic security for operations planning with significant wind power generation," *IEEE Trans. Power Syst.*, vol. 23, no. 2, pp. 306 - 316, May 2008.
- [12] Z.S. Zhang, Y.Z. Sun, G.-J. Li, L. Cheng, and J. Lin, "A solution of the economic dispatch problem considering wind power uncertainty," *Autom. Elect. Power Syst.*, vol. 35, no. 22, pp. 125 - 130, Nov. 2011.

- [13] N. Zhang, C. Kang, Q. Xia, and J Liang, "Modeling conditional forecast error for wind power in generation scheduling," *IEEE Trans. Power Syst.*, vol.29, no.3, pp. 1316-1324, May 2014.
- [14] A. Fabbri, T.G.S. Roman, J. R. Abbad, and V.H.M Quezada, "Assessment of the cost associated with wind generation prediction errors in a liberalized electricity market," *IEEE Trans. Power Syst.*, vol. 20, no. 3, pp. 1440 - 1446, Aug. 2005.
- [15] Y. V. Makarov, P. V. Etingov, J. Ma, Z. Y. Huang, and K. Subbarao, "Incorporating uncertainty of wind power generation forecast into power system operation, dispatch, and unit commitment procedures," *IEEE Trans. Sust. Energy*, vol. 2, no. 4, pp. 433 - 442, Oct. 2011.
- [16] Z. S. Zhang, Y. Z. Sun, D. W. Gao, J. Lin, and L. Cheng, "A versatile probability distribution model for wind power forecast errors and its application in economic dispatch," *IEEE Trans. Power Syst.*, vol. 28, no. 3, pp. 3114 - 3125, Aug. 2013.
- [17] J. Yan, Y. Q. Liu, S. Han, Y. M. Wang, et al, "Reviews on uncertainty analysis of wind power forecasting," *Renewable & Sustainable Energy Reviews*, vol. 52, pp. 1322-1330, December 2015.
- [18] J. Aghaei, T. Niknam, R. Azizipanah-Abarghooee, and J. M. Arroyo, "Scenario-based dynamic economic emission dispatch considering load and wind power uncertainties," *Int. J. Elect. Power & Energy Syst.*, vol. 47, pp. 351 - 367, May 2013.
- [19] J. Wang, A. Botterud, R. Bessa, H. Keko, L. Carvalho, D. Issicaba, J. Sumaili, V. Miranda, "Wind power forecasting uncertainty and unit commitment," *Applied Energy*, vol. 88, pp. 4014 4023, Nov. 2011.
- [20] B. Bahmani-Firouzi, E. Farjah, R. Azizipanah-Abarghooee, "An efficient scenario-based and fuzzy self-adaptive learning particle swarm optimization approach for dynamic economic emission dispatch considering load and wind power uncertainties," *Energy*, vol. 50, pp. 232 244, 2013.
- [21] A Botterud, Z Zhou, J Wang, et al, "Demand Dispatch and Probabilistic Wind Power Forecasting in Unit Commitment and Economic Dispatch: A Case Study of Illinois," *IEEE Transactions on Sustainable Energy*, vol. 4, no. 1, pp. 250 - 261, 2013.
- [22] A U Haque, M H Nehrir, P Mandal, "A Hybrid Intelligent Model for Deterministic and Quantile Regression Approach for Probabilistic Wind Power Forecasting," *IEEE Transactions on Power Systems*, vol. 29, no. 4, pp. 1663 – 1672, 2014.
- [23] J. Yan, Y. Q. Liu, S. Han, et al, "Wind power grouping forecasts and its uncertainty analysis using optimized relevance vector machine," *Renewable & Sustainable Energy Reviews*, vol. 27, pp. 613-621, 2013.
- [24] Y. Q. Liu, J. Yan, S. Han, D. Infield, et al, "An optimized short-term wind power prediction method considering NWP accuracy," *Chinese Science Bulletin.*, vol. 59, no. 11, pp. 1167 - 1175, April 2014.
- [25] P. Pinson, G. Papaefthymiou, B. Klöckl, H.A. Nielsen, H. Madsen, "From probabilistic forecasts to statistical scenarios of short-term wind power production," *Wind Energy*, vol. 12, no. 1, pp. 51-62, 2009.
- [26] M. E. Tipping, "Sparse Bayesian Learning and the Relevance Vector Machine," *Journal of Machine Learning Research*, vol. 1, pp. 211 - 244, 2001.
- [27] N S Rau, C Necsulescu, "Probability Distributions of Incremental Cost of Production & Production Cost," *IEEE Transactions on Power Apparatus & Systems*, vol. 104, no.12, pp. 3493 - 3500, 1986.
- [28] A Helander, Holttinen, et al, "Impact of wind power on the power system imbalances in Finland," *IET Renewable Power Generation*, vol. 4, no. 1, pp. 75 84, 2010.
- [29] Elexon Imbalance Pricing Guidance, [Online]. Available: http://www.elexon.co.uk/reference/credit-pricing/imbalance-pricing/.
- [30] N Zhang, C Kang, Q Xia, et al, "A Convex Model of Risk-Based Unit Commitment for Day-Ahead Market Clearing Considering Wind Power Uncertainty," *IEEE Transactions on Power Systems*, vol. 30, no. 3, pp. 1582 - 1592, 2014.